SuperScript II reverse transcriptase (GibcoBRL) and the anchored oligo-dT primer set (Genosys). The cDNA was than amplified by PCR. The SOD1 primers were from Genosys (forwards, 5′-ACGAAGGCCGTGTGCGTGCTGAA; backwards, 5′-ACCACAAGC-CAAACGACTTCCAGC). The reaction was run at 94 °C (1 min), 60 °C (1 min), 72 °C (1 min) for 20 cycles, which was within the linear reaction window. GAPDH was also measured by RT–PCR from the same RNA samples and used as an internal control (GAPDH primers: forwards, 5′-CCATCAATGACCCCTTCATTGACC; backwards, 5′-GAAGGCCATGCCAGTGAGCTTCC).

Assays of cellular accumulation and metabolism of 2-ME

To determine cellular uptake of 2-ME, cells were incubated with 1 μM [^{3}H]2-ME (0.5 μCi ml^{-1}) for 5 h and washed twice with cold PBS. Radioactivity associated with the cell pellets or the culture medium was quantified by liquid scintillation counting. 2-ME concentrations were calculated based on the specific radioactivity of [^{3}H]2-ME, cell number and the mean cell volume as measured by a Coulter Counter equipped with a 256-Channelyzer. We used HPLC to analyse potential cellular metabolites of 2-ME. Cells were incubated with [^{3}H]2-ME (0.5 μCi ml^{-1}) for 5 h, washed twice with PBS and then extracted with 50% methanol. The extracts were analysed by HPLC with an ultraviolet detector (284 nm) and an online liquid scintillation counter, using a μBondapak C_{18} reversed-phase column and the following running conditions: 1 ml min^{-1}; 0–5 min, 100% buffer A (water:acetontrile:acetic acid, 59:40:1); 5–26 min, a linear gradient of 0–100% buffer B (water:acetontrile:acetic acid, 39:60:1); 26–30 min, 100% buffer B.

Received 25 April; accepted 20 June 2000.

1. Halliwell, B. & Gutterridge, J. M. C. *Free Radicals in Biology and Medicine* (Oxford Univ. Press, New York, 1985).
2. Fridovich, I. Superoxide radical and superoxide dismutase. *Annu. Rev. Biochem.* **64,** 97–112 (1995).
3. Oberley, L. W. & Buettner, G. R. Role of superoxide dismutase in cancer: a review. *Cancer Res* **39,** 1141–1149 (1979).
4. Dionisi, O., Galeotti, T., Terranova, T. & Azzi, A. Superoxide radicals and hydrogen peroxide formation in mitochondria from normal and neoplastic tissues. *Biochim. Biophys. Acta* **403,** 292–300 (1975).
5. Marklund, S. L., Westman, N. G., Lundgren, E. & Roos, G. Copper- and zinc-containing superoxide dismutase, manganese-containing superoxide dismutase, catalase, and glutathione peroxidase in normal and neoplastic human cell lines and normal human tissues. *Cancer Res.* **42,** 1955–1961 (1982).
6. Van Driel, B. E. & Van Noorden, C. J. Oxygen insensitivity of the histochemical assay of glucose-6-phosphate dehydrogenase activity for the discrimination between nonmalignant and malignant cells. *J. Histochem. Cytochem.* **47,** 575–582 (1999).
7. Shulyakovskaya, T., Sumegi, L. & Gal, D. In vivo experimental studies on the role of free radicals in photodynamic therapy. I. Measurement of the steady state concentration of free radicals in tumor tissues of mice. *Biochem. Biophys. Res. Commun.* **95,** 581–587 (1993).
8. Cushman, M., He, H. -M., Katzenellenbogen, J. A., Lin, C. M. & Hamel, E. Synthesis, antitubulin and antimitotic activity, and cytotoxicity of analogs of 2-methoxyestradiol, an endogenous mammalian metabolite of estradiol that inhibits tubulin polymerization by binding to the colchicine binding site. *J. Med. Chem.* **38,** 2041–2049 (1995).
9. Mukhopadhyay, T. & Roth, J. A. Superinduction of wild-type p53 protein after 2-methoxyestradiol treatment of Ad5p53-transduced cells induces tumor cell apoptosis. *Oncogene* **17,** 241–246 (1998).
10. Fujimura, M. *et al.* Manganese superoxide dismutase mediates the early release of mitochondrial cytochrome *c* and subsequent DNA fragmentation after permanent focal cerebral ischemia in mice. *J. Neurosci.* **19,** 3414–3422 (1999).
11. Bindokas, V. J., Jordan, J., Lee, C. C. & Miller, R. J. Superoxide production in rat hippocampal neurons: selective imaging with hydroethidine. *J. Neurosci.* **16,** 1324–1336 (1996).
12. Ukeda, H., Maeda, S., Ishii, T. & Sawamura, M. Spectrophotometric assay for superoxide dismutase based on tetrazolium salt 3′-1-[(phenylamino)-carbonyl]-3,4-tetrazolium-bis(4-methoxy-6-nitro) benzenesulfonic acid hydrate reduction by xanthine-xanthine oxidase. *Anal. Biochem.* **251,** 206–209 (1997).
13. Zwacka, R. M., Dudus, L., Epperly, M. W., Greenberger, J. S. & Engelhardt, J. F. Redox gene therapy protects human IB-3 lung epithelial cells against ionizing radiation-induced apoptosis. *Hum. Gene Ther.* **9,** 1381–1386 (1998).
14. Heiden, M. G. V., Chandel, N. S., Williamson, E. K., Schumacker, P. T. & Thompson, C. B. Bcl-X_L regulates the membrane potential and volume homeostasis of mitochondria. *Cell* **91,** 627–637 (1997).
15. Marzo, I. *et al.* Bax and adenine nucleotide translocator cooperate in the mitochondrial control of apoptosis. *Science* **281,** 2027–2031 (1998).
16. Li, P. *et al.* Cytochrome *c* and ATP-dependent formation of Apaf-1/caspase-9 complex initiates an apoptotic protease cascade. *Cell* **91,** 479–489 (1997).
17. Rigo, A., Viglino, P. & Rotilio, G. Kinetic study of O_2^- dismutation by bovine superoxide dismutase: evidence for saturation of the catalytic sites by O_2^-. *Biochem. Biophys. Res. Commun.* **63,** 1013–1018 (1975).
18. D'Amato, R. J., Lin, C. M., Flynn, E., Folkman, J. & Hamel, E. 2-methoxyestradiol, an endogenous mammalian metabolite, inhibits tubulin polymerization by interacting at the colchicine site. *Proc. Natl Acad. Sci. USA* **91,** 3964–3968 (1994).
19. Fotsis, T. *et al.* The endogenous oestrogen metabolite 2-methoxyoestradiol inhibits angiogenesis and supresses tumor growth. *Nature* **368,** 237–239 (1994).
20. Gutteridge, J. M., Rowley, D. A. & Halliwell, B. Superoxide-dependent formation of hydroxyl radicals and lipid peroxidation in the presence of iron salts. Detection of 'catalytic' iron and anti-oxidant activity in extracellular fluids. *Biochem. J.* **206,** 605–609 (1982).
21. Hamana, K. *et al.* DNA strand scission by enzymatically reduced mitomycin C: evidence for participation of the hydroxyl radical in the DNA damage. *Biochem. Int.* **10,** 301–309 (1985).
22. Pervaiz, S., Ramalingam, J. K., Hirpara, J. L. & Clement, M. Superoxide anion inhibits drug-induced tumor cell death. *FEBS Lett.* **459,** 343–348 (1999).
23. Casppary, W. J, Niziak, C., Lanzo, D. A., Friedman, R. & Bachur, N. R. Bleomycin A2: a ferrous oxidase. *Mol. Pharmacol.* **16,** 256–260 (1979).
24. Young, R. C., Ozols, R. F. & Myers, C. E. The anthracycline antineoplastic drugs. *N. Engl. J. Med.* **305,** 139–153 (1981).
25. Gajewski, E., Rao, G., Nackerdien, Z. & Dizdaroglu, M. Modification of DNA bases in mammalian chromatin by radiation-generated free radicals. *Biochemistry* **29,** 7876–7882 (1990).
26. Mohanty, J. G., Jaffe, J. S., Schulman, E. S. & Raible, D. G. A highly sensitive fluorescent micro-assay of H_2O_2 release from activated human leukocytes using a dihydroxyphenoxazine derivative. *J. Immunol. Methods* **202,** 133–141 (1997).
27. Huang, P., Chubb, S. & Plunkett, W. Termination of DNA synthesis by 9-β-D-arabinofuranosyl-2-fluoroadenine: a mechanism for cytotoxicity. *J. Biol. Chem.* **265,** 16617–16625 (1990).

Acknowledgements

We thank J. Engelhardt and the Vector Core Facility of University of Iowa for Ad.CuZn-SOD, Ad.MnSOD and the control viral vectors; M. Du and A. Sandoval for technical assistance in the isolation and preparation of primary cells from health donors and from leukaemia patients; and J. Richard for editorial assistance. This work was supported in part by NIH/NCI grants to P.H. and W.P.

Correspondence and requests for materials should be addressed to P.H. (e-mail: phuang@notes.mdacc.tmc.edu).

A chemical switch for inhibitor-sensitive alleles of any protein kinase

Anthony C. Bishop*, Jeffrey A. Ubersax†, Dejah T. Petsch‡, Dina P. Matheos§, Nathanael S. Gray‖, Justin Blethrow†, Eiji Shimizu§, Joe Z. Tsien§, Peter G. Schultz‖, Mark D. Rose§, John L. Wood‡, David O. Morgan† & Kevan M. Shokat*¶

* *Department of Chemistry, Princeton University, Princeton, New Jersey 08544, USA*
† *Departments of Physiology and Biochemistry & Biophysics, University of California San Francisco, San Francisco, California 94143-0444, USA*
‡ *Department of Chemistry, Yale University, New Haven, Connecticut 06520-8107, USA*
§ *Department of Molecular Biology, Princeton University, Princeton, New Jersey 08544, USA*
‖ *Genomics Institute of the Novartis Research Foundation, San Diego, California 92121, USA*

Protein kinases have proved to be largely resistant to the design of highly specific inhibitors, even with the aid of combinatorial chemistry[1]. The lack of these reagents has complicated efforts to assign specific signalling roles to individual kinases. Here we describe a chemical genetic strategy for sensitizing protein kinases to cell-permeable molecules that do not inhibit wild-type kinases[2]. From two inhibitor scaffolds, we have identified potent and selective inhibitors for sensitized kinases from five distinct subfamilies. Tyrosine and serine/threonine kinases are equally amenable to this approach. We have analysed a budding yeast strain carrying an inhibitor-sensitive form of the cyclin-dependent kinase Cdc28 (CDK1) in place of the wild-type protein. Specific inhibition of Cdc28 *in vivo* caused a pre-mitotic cell-cycle arrest that is distinct from the G1 arrest typically observed in temperature-sensitive *cdc28* mutants[3]. The mutation that confers inhibitor-sensitivity is easily identifiable from primary sequence alignments. Thus, this approach can be used to systematically generate conditional alleles of protein kinases, allowing for rapid functional characterization of members of this important gene family.

Cell-permeable inhibitors that are selective for individual protein kinases would allow the direct investigation of the cellular function of each kinase in a pathway. Such molecules hold several advantages over genetic strategies for the disruption of kinase activity. Unlike gene deletions, drug-like inhibitors act quickly and reversibly, and

¶ Present address: Department of Cellular and Molecular Pharmacology, University of California San Francisco, San Francisco, CA 94143-0450, USA

do not allow the cell to compensate for the missing kinase activity during development. Likewise, highly specific inhibitors are preferable to temperature-sensitive alleles, as the analysis of temperature-sensitive phenotypes may be complicated by the effects of heat shock. In addition, the mechanism of temperature-sensitive protein inactivation is rarely understood in molecular detail.

We previously engineered the ATP-binding sites of Src-family tyrosine kinases to contain unique binding pockets that are not present in any wild-type protein kinase[2,4]. Mutation of Ile 338 to glycine in v-Src conferred unique inhibitor-sensitivity to chemically modified derivatives of PP1, the Src-family-selective inhibitor[2,5]. We reasoned that mutation of the equivalent position to a small amino acid may also confer unique inhibitor sensitivity in other protein kinase families. We therefore generated a series of rationally engineered protein kinases from divergent subfamilies. We selected at least one protein kinase from four distinct and physiologically important sub-families (Fig. 1a): Src family (v-Src, c-Fyn)[6,7], Abl family (c-Abl)[8], Ca^{2+}/calmodulin-dependent family (CAMK IIα)[9] and cyclin-dependent family (CDK2)[10]. The amino acid corresponding to residue 338 of v-Src was mutated to a small residue (glycine or alanine) for all of the above protein kinases to generate the following 'analogue-sensitive' (as) kinases: v-Src (I338G, v-Src-as1), c-Fyn (T339G, c-Fyn-as1), c-Abl (T315A, c-Abl-as2), CAMK IIα (F89G, CAMK IIα-as1) and CDK2 (F80G, CDK2-as1) (Fig. 1b; for c-Abl the T315G mutant, c-Abl-as1, was unstable; Y. Liu, personal communication). We then tested the mutation-dependent sensitivity of the analogue-sensitive kinases to two groups of derivatized inhibitors; one based on the indolocarbazole natural product (+)-K252a (Fig. 1c, **1**) and one based on PP1 (Fig. 1e).

K252a is a very general protein kinase inhibitor which we predicted would bind kinase active sites in an orientation identical to that of the closely related compound, staurosporine[11]. In the crystal structure of CDK2 bound to staurosporine, the F80 side chain is only 3.7 Å removed from C7 of staurosporine[11]. Thus, we anticipated that developing unique indolocarbazole-based inhibitors of our sensitized kinases would require selective manipulation of C7. We synthesized a small group of C7-derivatized K252a analogues[12] (Fig. 1c, **2**–**6**) and screened them against the wild-type and engineered protein kinases for *in vitro* inhibition of phosphorylation of an exogenous substrate (see Supplementary Information). The 2-methyl-propyl analogue (**3**) bound to the engineered Src-family kinases, v-Src-as1 and c-Fyn-as1, with high selectivity (≥ 3000-fold as compared with all wild-type kinases in the group) and subnanomolar half-maximal inhibitory concentration (IC_{50}) values (230 pM and 550 pM, respectively). These values represent the most potent inhibition of any Src-family kinase reported to date. Also, the 2-phenyl-ethyl derivative (**6**) is a potent and moderately selective inhibitor for the mutated CDK2 and CAMK IIα enzymes (see Supplementary Information). No selective inhibitors of c-Abl-as2 were identified from the K252a-based inhibitor group.

We next tested the same array of wild-type and mutant kinases against a group of C3-modified PP1 analogues[2] (Fig. 1e). Although PP1 is Src-family-selective, we reasoned that mutation of the 338

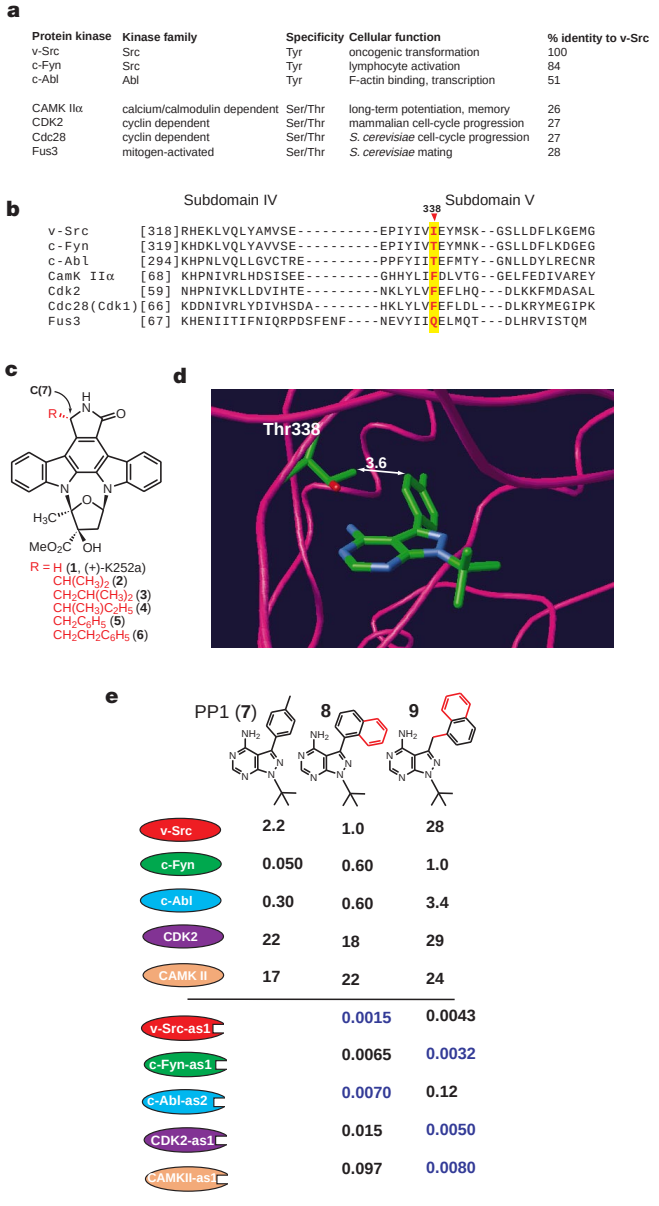

Figure 1 Structures of mutant kinase inhibitors. **a**, **b**, Substrate specificities, cellular functions, kinase domain sequence conservation and partial sequence alignment of the protein kinases. **c**, Chemical structures of (+)-K252a (**1**) and C7-derivatized K252a analogues (**2**–**6**). **d**, Crystal structure of PP1 bound to the Src-family tyrosine kinase Hck[29]. The Hck peptide backbone is shown as a magenta ribbon. The atoms of the Thr 338 side chain and PP1 are coloured as follows: carbon, green; nitrogen, blue; oxygen, red. **e**, Chemical structures of PP1 (**7**) and C3-derivatized PP1 analogues (**8**, **9**), and IC_{50} values (μM) for **7**–**9** against a group of wild-type and engineered protein kinases. IC_{50} values for the best K252a derivative/engineered kinase pair for each target are shown in blue.

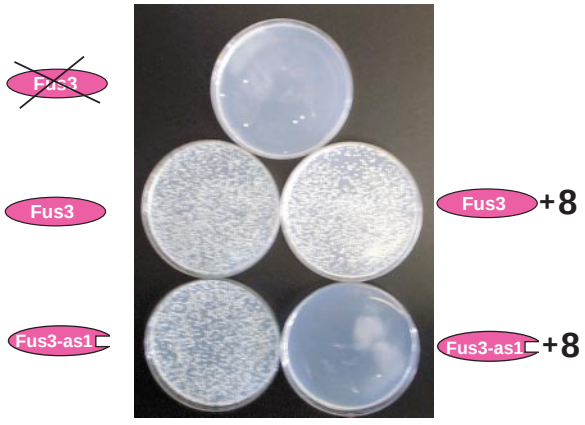

Figure 2 Selective disruption of *fus3-as1* yeast mating by analogue **8**. Haploid *URA3 his3 S. cerevisiae* expressing either wild-type Fus3, Fus3-as1, or no Fus3 were mated with an equal number of *ura3 HIS3 fus1*Δ *fus2*Δ cells and plated on media lacking uracil and histidine. Plates were inoculated with 0.1 ml of the mating cultures from the following strains (from top): *fus3*Δ; wild-type; wild-type + 5 μM analogue **8**; *fus3-as1*; *fus3-as1* + 5 μM analogue **8**.

position (v-Src numbering, Fig. 1d) to a small amino acid may confer unique PP1 analogue-sensitivity to other kinases, as this amino acid is partially responsible for the selectivity of PP1 itself[13].

Analysis of the PP1 analogue inhibition data (Fig. 1e) reveals some striking trends. PP1, which is much more selective than K252a (ref. 5), yielded analogues with wider utility in the context of the engineered kinase/inhibitor pairs. Each of the five target kinases was inhibited by PP1 analogues at low nanomolar concentrations with target-specificities ranging from 85-fold to 400-fold (measured against the most inhibitable wild-type kinase). There is little or no correlation between the wild-type PP1 IC_{50} and the PP1 analogue sensitivity of the same (engineered) kinase. This is most apparent in the Ser/Thr kinases CDK2 and CAMK IIα. These wild-type enzymes both possess weak PP1 IC_{50} values of greater than 15 μM. However, both CDK2-as1 and CAMK IIα-as1 are very potently inhibited by the C3-1′-naphthylmethyl PP1 analogue (**9**; 5.0 nM and 8.0 nM, respectively). This dichotomy is most probably due to a combination of the importance of residue 338 in determining the PP1 sensitivity of a given protein kinase[13], and the affinity of the naphthyl ring system for the expanded kinase active site[2]. The IC_{50} values for analogue **9** for all of the glycine mutants were within a threefold range (all < 10 nM) of each other even though their wild-type PP1 sensitivities vary by more than 400-fold. None of the wild-type kinases tested are inhibited at concentrations of less than 1 μM **9**, showing the high target-selectivity of this compound (Fig. 1e).

The PP1 analogues **8** and **9** are selective for different space-creating mutations on the basis of their size and flexibility. The more rigid C3-1′-naphthyl PP1 analogue (**8**) shows a broader range of potency between different kinase glycine mutants (Fig. 1e); however, it potently inhibits c-Abl-as2 (7.0 nM) with high specificity. In addition, **8** inhibits the alanine mutant of v-Src (I338A, v-Src-as2; IC_{50} = 1.0 nM) more strongly than it inhibits the corresponding glycine mutant, suggesting that this molecule will provide a general scheme for the development of monospecific inhibitors for protein kinases whose activity or stability is significantly compromised by the glycine mutation.

We then investigated whether our strategy could be used to generate inhibitor-sensitive kinase alleles with *in vivo* utility. PP1 analogues can be used for target-specific inhibition of retrovirally expressed v-Src in murine fibroblasts[2]. We were interested, however, in showing monospecific inhibition of endogenous kinase gene products in an organism that has broad utility in traditional genetic

a

Kinase	ATP kinetics K_M (μM)	ATP kinetics k_{cat} (min^{-1})	ATP kinetics k_{cat}/K_M ($\mu M^{-1}min^{-1}$)	IC_{50} (μM 9) @ 10 μM ATP	IC_{50} (μM 9) @ 1 mM ATP
Cdc28/Clb2	35	132	3.730	22	44
Cdc28-as1/Clb2	322	21.3	0.066	.0020	.0029

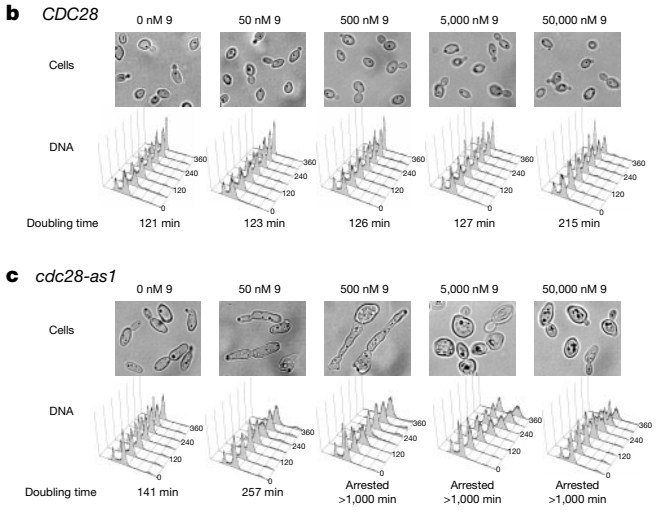

Figure 3 Characterization of the cdc28-as1 mutant. **a**, Cdc28-as1 is highly sensitive to analogue **9** *in vitro* and is a slightly weakened kinase. **b**–**c**, The *cdc28-as1* strain is highly sensitive to **9** and displays several cell-cycle arrest points upon inhibitor addition. *CDC28* and *cdc28-as1* strains were grown to mid-log phase and resuspended in fresh media containing the indicated concentration of **9**. Samples were taken at the indicated times and fixed for microscopy, flow cytometric analysis and cell counting. The cell micrographs shown were taken 5 h after addition of compound **9**.

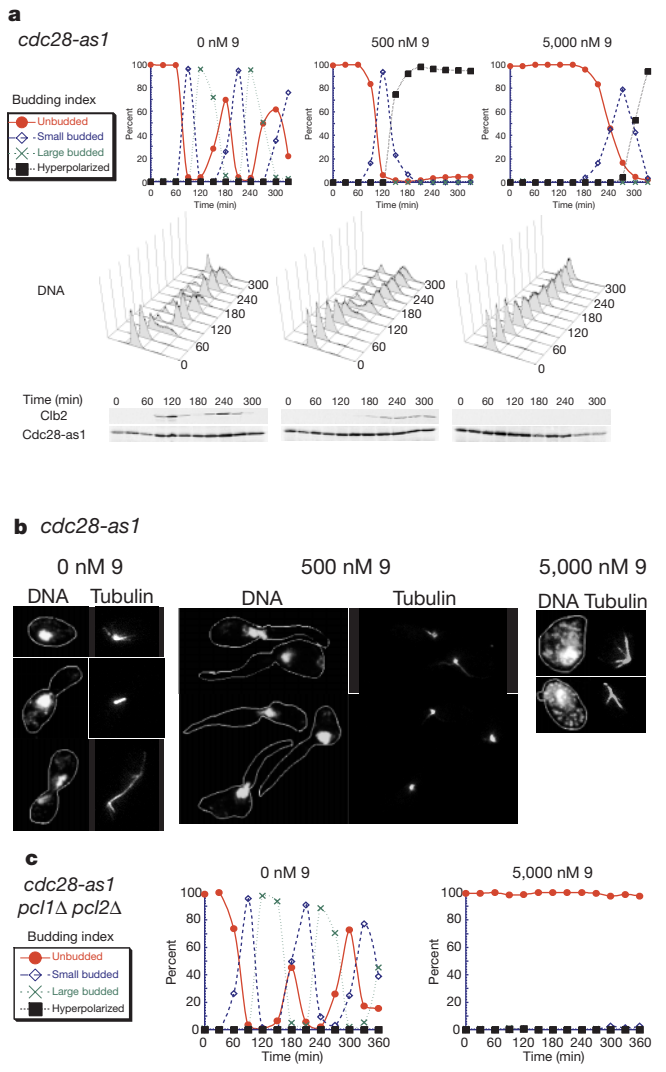

Figure 4 Characterization of cdc28-as1 phenotype at different concentrations of analogue **9**. **a**, *cdc28-as1* cells synchronized in G1 and released into analogue **9** display a G2/M arrest (500 nM) and a G1 arrest (5,000 nM). *cdc28-as1* strains were arrested in G1 by 1 μg ml^{-1} α-factor for 2.5 h. Indicated concentrations of **9** were added for 20 min, and cells were released from G1 by washing and resuspension in media containing the same concentration of **9**. Every 30 min, samples were fixed for analysis of budding index and flow cytometry as in Fig. 3. Parallel samples were analysed by western blotting for Clb2 and Cdc28. **b**, *cdc28-as1* cells arrest either before mitotic entry with no mitotic spindle (500 nM) or in a G1-like state with an interphase microtubule array (5,000 nM). *cdc28-as1* cells were arrested in G1 and released as above. Cells are shown 240 min after release, except those released into 0 nM **9**, where cells were taken at 180 (top), 210 (middle) and 240 (bottom) min after release to show normal spindle morphology during the cell cycle. Tubulin and DNA staining were done as described[30]. **c**, Budding of cells released from G1 into 5,000 nM **9** is due to Pho85/Pcl1-2 activity. G1 synchronization, release and budding indices were done as above in a *cdc28-as1 pcl1Δ::HIS3 pcl2Δ::URA3* strain.

screens. The budding yeast, *Saccharomyces cerevisiae*, is widely used as a unicellular model organism in genetic studies as it is susceptible to genetic manipulation and grows rapidly. The *S. cerevisiae* genome encodes over 120 protein kinases including homologues of proteins from many mammalian kinase families[14]. Ideally, the kinase-sensitization strategy could be extended to these protein kinases without individually purifying and assaying every enzyme *in vitro*. To test this idea, we selected the *S. cerevisiae* MAP kinase Fus3, which is required for induction of pheromone-inducible genes, cell-cycle arrest and cell fusion during yeast mating[15]. No temperature-sensitive alleles of Fus3 have been isolated, possibly because of the temperature sensitivity of the mating process[16].

We mutated Gln 93 of *FUS3* (corresponding to I338 in v-Src) to glycine (Fus3-as1), and expressed this enzyme in budding yeast that lack wild-type Fus3. The *fus3-as1* mutant fully complemented the gene deletion, as shown by the mating of equal numbers of haploid wild-type or *fus3-as1* cells (*URA3 his3*) to a *fus1*Δ *fus2*Δ *ura3 HIS3* strain followed by selection for diploid progeny on media lacking uracil and histidine. Wild-type and *fus3-as1* strains both yielded about 7.5×10^4 colony-forming units (c.f.u.) per ml while mating of a *fus3*Δ strain gave only 0–100 c.f.u. per ml under the same selection conditions. When the mating of a *fus3-as1* strain was carried out in the presence of 50 μM or 5 μM **8**, the number of diploids formed was indistinguishable from a *fus3*Δ strain (Fig. 2). Even at 500 nM **8**, the *fus3-as1* strain gave only 1.7×10^3 c.f.u. per ml, a 44-fold decrease from equivalent control cells. Because of the competition with millimolar quantities of ATP in the yeast cell, this strong inhibition at 500 nM analogue **8** implies an *in vitro* IC_{50} for Fus3-as1 in the low nanomolar range[2]. Analogue **9** also disrupted mating in *fus3-as1* cells, but with less potency (see Supplementary Information). By contrast, no decrease in mating efficiency was observed when wild-type cells were treated with **8** or **9** ($(0.6–1.1) \times 10^5$ c.f.u. per ml at all concentrations up to 50 μM). Therefore *fus3-as1* represents the first conditional allele of this MAP kinase. Through the *in vivo* addition of analogue **8**, the activity of the Fus3 kinase can be controlled selectively, rapidly and in a dose-dependent fashion.

We next set out to use PP1 analogues to study the *S. cerevisiae* cell cycle through selective inhibition of the protein kinase Cdc28. This enzyme is the principal CDK in budding yeast and is essential for progression through several stages of the cell cycle[17]. The function of Cdc28 has been studied primarily by the analysis of temperature-sensitive mutant alleles[3]. At 37 °C, most of these mutants arrest in G1, suggesting that progression through START (the G1 commitment point) is sensitive to inhibition of Cdc28 activity. Notably, analysis of temperature-sensitive mutants has not provided clear evidence that Cdc28 is involved in the G2/M transition, despite abundant evidence that CDK1 is required for mitotic entry in other eukaryotes[18]. One well-studied temperature-sensitive mutant of *CDC28*, *cdc28-1N*, exhibits a metaphase arrest at the restrictive temperature[19]; however, both structural and biochemical data have suggested that the arrest of *cdc28-1N* cells is due to a temperature-sensitive protein–protein interaction (with Cks1), and not a general block of Cdc28 kinase activity[19,20].

Cdc28 is 62% identical to human CDK2, suggesting that the engineered Cdc28, Cdc28-as1 (F88G) should be susceptible to inhibition by C3-derivatized PP1 analogues. We expressed and purified Cdc28–His_6 and Cdc28-as1–His_6 from Sf9 insect cells, and formed active complexes with bacterially expressed MBP–Clb2.

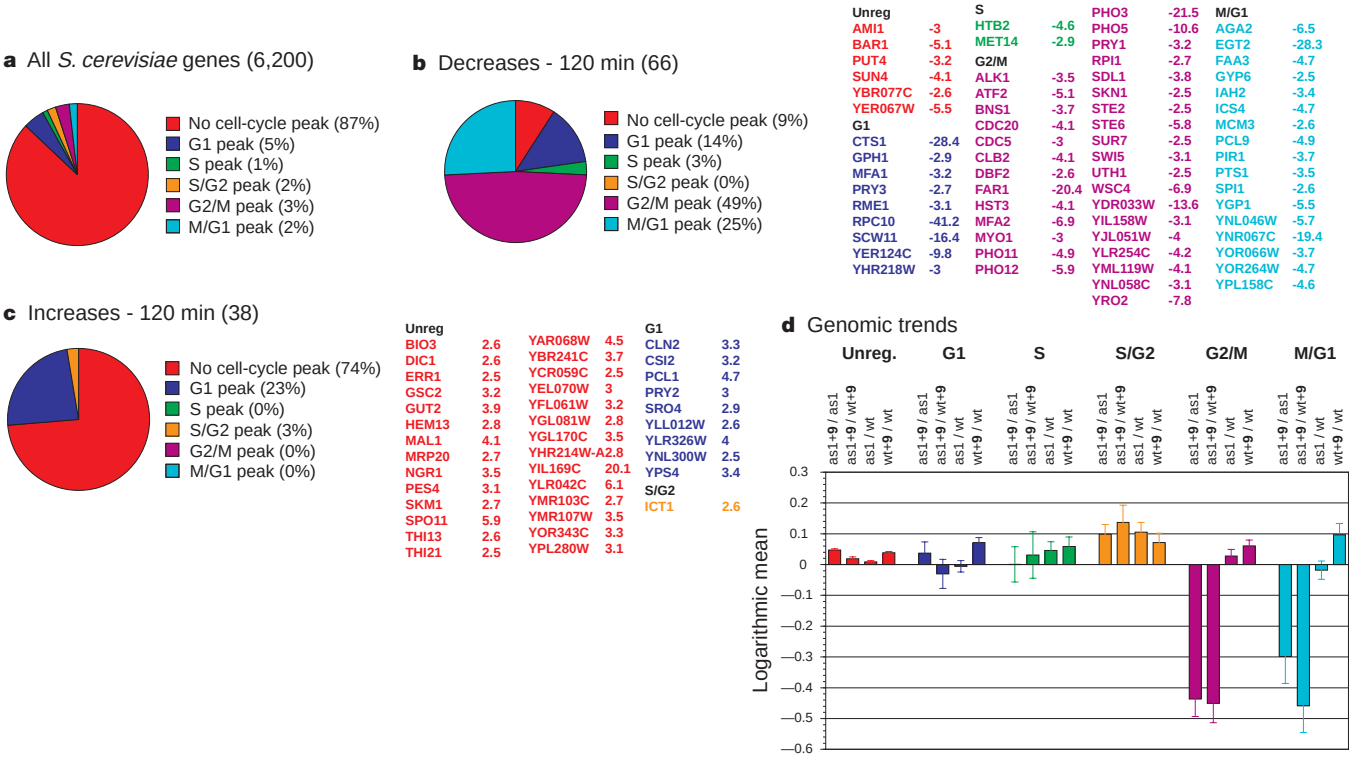

Figure 5 Treatment with 500 nM **9** leads to a drop in G2/M transcription. **a**, For comparison, this chart shows the percentage of genes whose transcription is known to be regulated during the cell cycle[23]. **b**, **c**, Asynchronous *cdc28-as1* cells were treated with 500 nM **9** for 120 min. Genome-wide transcriptional differences ± **9** were measured by oligonucleotide microarray analysis of cellular mRNA[21]. **b**, Transcripts that decreased over 2.5-fold after treatment with **9**. **c**, Transcripts that increased over 2.5-fold after treatment with **9**. Transcripts are grouped in the lists and pie charts according to their known cell-cycle regulation[23]. **d**, Genome-wide changes in transcription were assessed in four comparisons as follows: 1, *cdc28-as1* cells + 500 nM **9** versus untreated *cdc28-as1* cells (as1+**9** / as1); 2, drug-treated *cdc28-as1* cells versus drug-treated wild-type cells (as1+**9** / wt+**9**); 3, untreated *cdc28-as1* cells versus wild-type cells (as1 / wt); and 4, drug-treated wild-type cells versus untreated wild-type cells (wt+**9** / wt). For each comparison, the natural log of the ratio of gene expression under the two conditions was used to calculate the mean logarithmic change in expression of all G1, S, S/G2, G2/M, M/G1 and non-cell-cycle-regulated (Unreg.) genes. Error bars represent the s.e.m.

Relative to wild-type Cdc28, Cdc28-as1 displayed a moderate reduction in activity, including a tenfold reduction in ATP-binding affinity and a sixfold reduction in maximum ATP turnover rate (Fig. 3a). More notably, Cdc28-as1 was highly sensitive to **9**. In 1 mM ATP, which approximates intracellular ATP concentration, Cdc28-as1 was about 15,000-fold more sensitive to **9** than was wild-type Cdc28 ($IC_{50} \approx 3$ nM for Cdc28-as1, and 44,000 nM for Cdc28). Thus, the single substitution of a glycine for a phenylalanine results in a Cdc28 mutant that displays both high affinity and specificity for analogue **9**.

To examine the function of Cdc28 *in vivo*, we constructed a yeast strain in which the wild-type copy of *CDC28* was replaced by *cdc28-as1*. In the absence of **9**, *cdc28-as1* cells displayed normal viability and growth on plates, although they were hyperpolarized and larger than an isogenic *CDC28* strain, and had a 20% longer doubling time in liquid culture (Fig. 3b, c). Flow cytometric analysis of asynchronously dividing cells revealed that the *cdc28-as1* and *CDC28* strains displayed similar DNA content profiles (Fig. 3b, c). We also used synthetic oligonucleotide DNA arrays to measure genome-wide transcriptional differences between asynchronous wild-type and *cdc28-as1* cells[21]. In two separate experiments, greater than twofold changes were observed in only 11 transcripts (0.2% of the genome).

We suspect that the minor growth defect in *cdc28-as1* cells is due to the sixfold lower catalytic rate constant (k_{cat}) of the mutant enzyme, which would result in a sixfold lower activity at the high ATP concentrations *in vivo* (the lower ATP-binding affinity of the mutant should not be relevant *in vivo*, where ATP concentration is much greater than the Michaelis constant, K_m). Thus, *cdc28-as1* is a slightly weakened allele of *CDC28*, but can support cell-cycle progression.

We analysed the effects of analogue **9** on cell growth and morphology. Proliferation of wild-type cells was unaffected by the inhibitor except at very high concentrations (50,000 nM), when doubling times increased about twofold (Fig. 3b). Hybridization to oligonucleotide arrays revealed that transcription of only six genes (0.1%) was changed more than twofold after 30 min treatment of wild-type cells with 500 nM compound **9**. Treatment of cells for 120 min caused even fewer transcriptional responses: only three transcripts showed more than twofold changes. No significant activation of stress-responsive transcripts was observed. We conclude that treatment with 500 nM compound **9** has no significant effects on wild-type cell physiology.

The single amino-acid change in the Cdc28-as1 kinase makes it very sensitive to **9** *in vivo*. Growth of the *cdc28-as1* strain was inhibited 50% at 50–100 nM **9**; complete growth arrest occurred at 500 nM **9** (Fig. 3c). The close correspondence between the IC_{50} *in vivo* and those measured in kinase assays (Fig. 3a) illustrates the efficacy with which **9** can penetrate a yeast cell, a feature not shown by other small-molecule CDK inhibitors[1].

Analysis of DNA content and morphology of *cdc28-as1* cells showed that lower concentrations of **9** caused a delay (50 nM) or arrest (500 nM) with a G2/M DNA content and large hyperpolarized buds (Fig. 3c). Higher inhibitor concentrations (5,000 nM) caused a non-uniform arrest that included unbudded G1 cells as well as large-budded G2/M cells; bud hyperpolarization was no longer evident. The *cdc28-as1* mutant phenotype is recessive: the inhibitor had no effect in diploid cells carrying both a wild-type *CDC28* gene and a *cdc28-as1* mutant allele (data not shown). Thus, the effects of **9** in *cdc28-as1* cells are not due to dominant-negative effects of inactive kinase complexes in the cell.

When *cdc28-as1* cells were synchronized in G1 with the yeast mating pheromone, α-factor, and released into fresh media containing 500 nM **9**, initiation of budding and DNA synthesis was delayed about 30–60 min, and accumulation of the mitotic cyclin Clb2 was delayed 60–90 min (Fig. 4a). Cells went on to arrest with moderate Clb2 levels, highly hyperpolarized buds and a G2/M DNA content, much like the arrest observed in asynchronous cells. Microscopic analysis of microtubules and DNA revealed that these cells lacked a mitotic spindle and arrested with a single DNA mass correctly positioned at the bud neck (Fig. 4b). Cells treated with low concentrations of the inhibitor are therefore slightly delayed during progression through early stages of the cell cycle, and eventually arrest because of a failure to assemble a mitotic spindle and enter mitosis.

When we released G1-synchronized *cdc28-as1* cells into media containing 5,000 nM **9**, they arrested with a 1*C* DNA content (unreplicated DNA) and initially failed to bud, suggesting an arrest at START (this arrest was reversible, as washing away the inhibitor after 60 min allowed cells to rapidly resume a normal cell cycle; see Supplementary Information). Arrested cells eventually budded after 180–240 min of inhibitor treatment, and arrested with a 1*C* DNA content, large hyperpolarized buds, a single DNA mass in the mother cell, an interphase astral microtubule array and no detectable Clb2 (Fig. 4a, b).

Pho85, a CDK that is closely related to Cdc28, has been implicated in the initiation of budding in *S. cerevisiae*[22]. We therefore investigated whether the budding that we observed in *cdc28-as1* cells released into 5,000 nM **9** was due to residual Cdc28-as1 or Pho85 activity. We constructed a *cdc28-as1* strain lacking *PCL1* and *PCL2*, which encode the two G1 activating cyclins of Pho85. When these cells were synchronized in G1 and released into 5,000 nM **9**, they arrested with a 1*C* DNA content and did not bud, even after 6 h (Fig. 4c). We conclude that Pcl1- and Pcl2-associated Pho85 activities, and not residual Cdc28 activity, are responsible for the greatly delayed budding observed in *cdc28-as1* cells treated with high concentrations of inhibitor.

To characterize further the cell-cycle arrest caused by inhibitor treatment, we analysed genome-wide transcription after treatment of asynchronous *cdc28-as1* cells with 500 nM **9** (Fig. 5). Treatment for 2 h caused 2.5-fold or greater changes in the transcription of 104 genes (66 decreases, 38 increases) (Fig. 5b, c). Of the downregulated transcripts, 60 are cell-cycle-regulated and 32 have peak expression at G2/M[23]. This downregulated G2/M subset contains a broad range of well-established mitotic regulators, including *CLB2*, *SWI5*, *CDC20* and *CDC5*. Decreased levels of the *CLB2* transcript are consistent with the delay in Clb2 accumulation after release from G1 arrest (Fig. 4a). Treatment with **9** for 30 min produced a similar G2/M transcriptional block (37 of the 42 downregulated genes are cell-cycle regulated, and 57% of these peak at G2/M; see Supplementary Information), suggesting that the inhibitor reaches active intracellular concentrations within minutes after addition to the growth media.

Two-hour drug exposure also increased the expression of 38 transcripts over 2.5-fold (10 cell-cycle regulated) (Fig. 5c). Nine of the ten cell-cycle regulated transcripts are expressed at peak levels in G1. This group includes genes encoding G1 cyclins (Cln2, Pcl1). This result, combined with the fact that the Cln–Cdc28 inhibitor Far1 was downregulated 20-fold, suggests that prolonged Cdc28 inhibition and G2/M arrest lead to a transcriptional program that boosts the activity of G1 cyclin/CDK complexes.

To assess general trends in the transcriptional response to Cdc28 inhibition, we also calculated mean changes in the expression of all genes from each of the principal cell-cycle gene clusters (Fig. 5d). This analysis confirmed that inhibitor treatment of *cdc28-as1* cells led primarily to decreased expression of genes that are normally expressed in the G2/M and M/G1 stages of the cell cycle.

We conclude that low concentrations of **9** cause *cdc28-as1* cells to arrest before mitosis with a phenotype similar to that observed in cells lacking the mitotic cyclins Clb1–Clb4 (ref. 24). Entry into mitosis appears particularly sensitive to inhibition of Cdc28 catalytic activity, and only at higher concentrations of inhibitor does complete inhibition of passage through G1 occur. These data are generally consistent with the idea that different cell-cycle events are triggered by specific threshold levels of CDK activity, and that later

events require higher amounts of activity[25].

Our results do not seem consistent with previous studies[3,17] of temperature-sensitive *cdc28* mutants, most of which arrest as unbudded cells in G1. One explanation for this discrepancy is that there are major differences in the inhibitor sensitivity of different Cdc28/cyclin complexes. We have been unable to test this possibility directly because we find that Cdc28-as1/Cln complexes exhibit insufficient activity *in vitro* to allow detailed analysis of their inhibitor-sensitivity (data not shown). Nevertheless, it seems unlikely that Cdc28-as1/Cln complexes exhibit significantly reduced sensitivity to **9**, given that four different as1 kinase mutants (from three different kinase families) displayed roughly the same nanomolar sensitivity that we observed for Cdc28-as1/Clb2 (Figs 1 and 3a).

Using a chemical switch to design a unique protein/small molecule interface we can systematically engineer protein kinases with unique sensitivity to cell-permeable inhibitors. This approach can be successful even for protein kinases that are not potently inhibited by the chosen 'lead' inhibitor, and different small-molecule scaffolds can be used to generate analogues that are specific for the same target. Developing several chemical structures for inhibition of a specific target may prove valuable for application of this kinase-sensitization strategy to mammalian studies, as bio-availability and selectivity requirements (>1000 protein kinases) become more stringent. Our data suggest that most protein kinases will be susceptible to this target-specific inhibition strategy. For organisms that readily undergo homologous recombination, this approach raises the possibility of generating conditional allelic strains for every protein kinase in the genome. A library of such strains would represent a significant step forward in realizing the pharmacogenomic vision of identifying small-molecule ligands for every gene product in the cell. □

Methods

Chemical synthesis

(+)-K252a (ref. 12) and PP1 (ref. 2) analogues were synthesized as described.

Protein expression and purification

Wild-type and engineered GST–v-Src (catalytic domain), GST–c-Fyn, GST–c-Abl, GST–CAMK IIα and CDK2–His_6 were expressed and purified as described[13].

Lysate was prepared from insect cells co-infected with baculoviruses encoding Cdc28–His_6 or Cdc28-as1–His_6 and Cak1-HA_3 (ref. 26). Cdc28-His_6 and Cdc28-as1–His_6 were purified by metal-affinity, followed by anion-exchange (Pharmacia SP Sepharose Fast Flow) and cation-exchange (Pharmacia Q Sepharose Fast Flow) chromatography. MBP–Clb2 was purified from lysates of bacteria expressing MBP–Clb2 (a gift from R. Deshaies).

Yeast plasmid and strain construction

Genetic and microbial techniques were done essentially as described[27]. To generate a plasmid containing *FUS3*, we constructed plasmid pMR3980 by cloning an *Eco*RI/*Pml*I fragment from pMR2412 into pRS416 (ref. 28) cut with *Eco*RI/*Sma*I. The Q93G mutant allele, pMR4280, was created by phagemid *in vitro* mutagenesis of plasmid pMR3980. Strain MY2914, MAT*a*/*fus3*Δ::*LEU2*, was transformed with either pMR3980, pMR4280 or pRS416.

All *CDC28* strains were derivatives of W303 (*ura3-1, leu2-3,112, trp1-1, his3-11,15, ade2-1, can1-100, GAL*+). To create *cdc28-as1*, the *CDC28* coding sequence and 400 bp of 5′- and 386 bp of 3′ flanking DNA were PCR-amplified from genomic DNA and ligated into pRS306 (ref. 28) to make pJAU1. The F88G mutation was engineered by oligonucleotide-directed mutagenesis of pJAU1. The plasmid was integrated into the wild-type *CDC28* locus following *Afl*II digestion by a pop-in–pop-out strategy as described[27].

In vitro kinase assays

We carried out *in vitro* kinase assays (except for Cdc28) in the presence of 0.2 μCi μl^{-1} [γ-^{32}P]ATP at low ATP concentration (10 nM) so that IC_{50} values represent a rough measure[13] of the inhibition constant (K_i). Measurement of inhibitor IC_{50} values were done as described[13].

Purified Cdc28–His_6 (1 nM) and MBP–Clb2 (3 nM) were incubated for 10 min at 23 °C in a 25 μl reaction mixture containing 5 μg histone H1, 1 μCi of [γ-^{32}P]ATP (1 μCi per 10 μM and 1 μCi per 1 mM), and varying concentrations of compound **9** in kinase buffer (25 mM HEPES-NaOH pH 7.4, 10 mM NaCl, 10 mM $MgCl_2$ and 1 mM dithiothreitol). Reaction products were analysed by 15% SDS–PAGE followed by autoradiography. For the determination of Cdc28 kinetic constants, varying concentrations of [γ-^{32}P]ATP (1 μCi per 100 μM) were incubated and analysed as above.

Fus3-dependent mating assays

Haploid *URA3 his3 S. cerevisiae* expressing either wild-type Fus3, Fus3-as1, or no Fus3 at an absorbance of 0.5 at 600 nm were mated with an equal number of *ura3 HIS3 fus1*Δ *fus2*Δ cells and pipetted onto a nitrocellulose disk. The disk was placed on a YPD plate containing varying amounts amount of inhibitor for 5 h at 30 °C. Cells were liberated and dilutions of the resulting cultures were plated on media lacking uracil and histidine and grown at 30 °C and the colonies were counted. All cultures were also plated on YPD media. No significant decrease in c.f.u. per ml on YPD plates was observed for any of the three strains in the presence of analogue **8** or **9**.

DNA flow cytometry

Roughly 10^7 cells for each sample were fixed in 70% ethanol, resuspended in 50 mM Tris-HCl pH 8.0, briefly sonicated, digested with 2 mg ml^{-1} RNase for 2 h at 37 °C, and resuspended in 0.2 ml protease solution (5 mg ml^{-1} pepsin, 0.5% concentrated HCl) and digested for 45 min at 37 °C. We stained DNA with 1 μM Sytox Green (Molecular Probes) in 50 mM Tris-HCl pH 7.5, and scanned 20,000 cells from each sample with a FACScan machine (Becton-Dickinson).

Genome-wide transcriptional analysis

We measured genome-wide transcriptional differences by oligonucleotide microarray analysis of cellular messenger RNA as described[21]. Changes were deemed significant if they were greater than or equal to 2.0-fold or if the transcript changed present/absent status (as indicated by Affymetrix software) in the following comparisons: for nonspecific drug effects, *CDC28* + **9** versus *CDC28*; for *cdc28-as1* effects, *cdc28-as1* versus *CDC28*. For specific Cdc28 inhibition effects, changes were deemed significant if they were equal to or greater than 2.5-fold for *cdc28-as1* + **9** versus *cdc28-as1* and also greater than or equal to 2.0-fold for *cdc28-as1* + **9** versus *CDC28* + **9**.

Greater than twofold differences were observed in expression of the following genes in a comparison of wild-type and *cdc28-as1* cells (11 overlaps between the 2 experiments are underlined). Experiment 1: *LEU2*, YDL241W, YFL057C, YHR071W, *CBP1*, YJR130C, *CWP1*, YLL060C, *ATR1*, YML128C, YMR095C, YMR096W, YNL275W, YNR065C, *ARG1*, YOL101C, *SPS4*, *SSU1*, *SVS1*, *OYE3*, *RLF2* and YPR203W. Experiment 2: *DUR1*, *CIT2*, YDL241W, *INO2*, YFL056C, YFL057C, YGL088W, YHR071W, *TWT1*, YHR209W, YIL011W, YIL023C, *DAL4*, YKL218C, YLL060C, YLR108C, YLR237W, YLR437C, YML071C, *ATR1*, YMR095C, YMR096W, YNR065C, *ARG1*, YOR302W, *SPS4*, YPL088W, *SVS1*, YPR013C and *CTR1*.

Of the six transcripts that changed in wild-type cells after 30 min of 500 nM inhibitor treatment, three have no known function (YGR035C, YLR346C, YPL222W) and the others have roles in heat shock (*SSA4*), osmotic stress response (*GRE2*) and drug resistance (*YOR1*). The transcription of only one of these genes (YGR035C) is cell-cycle regulated[23]. Treatment of wild-type cells with 500 nM inhibitor for 120 min resulted in changes in only three genes (YGR035C and two genes encoding ribosomal proteins: *RPS26A* and *RPL26B*).

Received 26 April; accepted 24 July 2000.

1. Gray, N. S. *et al.* Exploiting chemical libraries, structure, and genomics in the search for kinase inhibitors. *Science* **281,** 533–538 (1998).
2. Bishop, A. C. *et al.* Generation of monospecific nanomolar tyrosine kinase inhibitors via a chemical genetic approach. *J. Am. Chem. Soc.* **121,** 627–631 (1999).
3. Reed, S. I. The selection of *S. cerevisiae* mutants defective in the start event of cell division. *Genetics* **95,** 561–577 (1980).
4. Liu, Y., Shah, K., Yang, F., Witucki, L. & Shokat, K. M. Engineering Src family protein kinases with unnatural nucleotide specificity. *Chem. Biol.* **5,** 91–101 (1998).
5. Hanke, J. H. *et al.* Discovery of a novel, potent, and Src family-selective tyrosine kinase inhibitor. *J. Biol. Chem.* **271,** 695–701 (1996).
6. Brown, M. T. & Cooper, J. A. Regulation, substrates and functions of src. *Biochim. Biophys. Acta* **1287,** 121–149 (1996).
7. Resh, M. D. Fyn, a Src family tyrosine kinase. *Int. J. Biochem. Cell Biol.* **30,** 1159–1162 (1998).
8. Laneuville, P. Abl tyrosine protein kinase. *Semin. Immunol.* **7,** 255–266 (1995).
9. Kelly, P. T. Calmodulin-dependent protein kinase II. Multifunctional roles in neuronal differentiation and synaptic plasticity. *Mol. Neurobiol.* **5,** 153–177 (1991).
10. Morgan, D. O. Principles of CDK regulation. *Nature* **374,** 131–134 (1995).
11. Lawrie, A. M. *et al.* Protein kinase inhibition by staurosporine revealed in details of the molecular interaction with CDK2. *Nature Struct. Biol.* **4,** 796–801 (1997).
12. Wood, J. L., Stoltz, B. M., Dietrich, H. J., Pflum, D. A. & Petsch, D. T. Design and implementation of an efficient synthetic approach to furanosylated indolocarbazoles: total synthesis of (+)- and (−)-K252a. *J. Am. Chem. Soc.* **119,** 9641–9651 (1997).
13. Liu, Y. *et al.* Structural basis for selective inhibition of Src family kinases by PP1. *Chem. Biol.* **6,** 671–678 (1999).
14. Hunter, T. & Plowman, G. D. The protein kinases of budding yeast: six score and more. *Trends Biochem. Sci.* **22,** 18–22 (1997).
15. Fujimura, H. A. Yeast homolog of mammalian mitogen-activated protein kinase, Fus3/Dac2 kinase, is required both for cell fusion and for G1 arrest of the cell cycle and morphological changes by the cdc37 mutation. *J. Cell. Sci.* **107,** 2617–2622 (1994).
16. Doi, S. & Yoshimura, M. Temperature-sensitive loss of sexual agglutinability in *Saccharomyces cerevisiae*. *Arch. Microbiol.* **114,** 287–288 (1977).
17. Mendenhall, M. D. & Hodge, A. E. Regulation of Cdc28 cyclin-dependent protein kinase activity during the cell cycle of the yeast *Saccharomyces cerevisiae*. *Microbiol. Mol. Biol. Rev.* **62,** 1191–1243 (1998).
18. King, R. W., Jackson, P. K. & Kirschner, M. W. Mitosis in transition. *Cell* **79,** 563–571 (1994).
19. Surana, U. *et al.* The role of CDC28 and cyclins during mitosis in the budding yeast *S. cerevisiae*. *Cell* **65,** 145–161 (1991).

20. Bourne, Y. *et al.* Crystal structure and mutational analysis of the human CDK2 kinase complex with cell cycle-regulatory protein CksHs1. *Cell* **84,** 863–874 (1996).
21. Wodicka, L., Dong, H., Mittmann, M., Ho, M. H. & Lockhart, D. J. Genome-wide expression monitoring in *Saccharomyces cerevisiae*. *Nature Biotechnol.* **15,** 1359–1367 (1997).
22. Espinoza, F. H., Ogas, J., Herskowitz, I. & Morgan, D. O. Cell cycle control by a complex of the cyclin HCS26 (PCL1) and the kinase PHO85. *Science* **266,** 1388–1391 (1994).
23. Spellman, P. T. *et al.* Comprehensive identification of cell cycle-regulated genes of the yeast *Saccharomyces cerevisiae* by microarray hybridization. *Mol. Biol. Cell* **9,** 3273–3297 (1998).
24. Fitch, I. *et al.* Characterization of four B-type cyclin genes of the budding yeast *Saccharomyces cerevisiae*. *Mol. Biol. Cell* **3,** 805–818 (1992).
25. Stern, B. & Nurse, P. A quantitative model for the cdc2 control of S phase and mitosis in fission yeast. *Trends Genet.* **12,** 345–350 (1996).
26. Farrell, A. & Morgan, D. O. Cdc37 promotes the stability of protein kinases Cdc28 and Cak1. *Mol. Cell. Biol.* **20,** 749–754 (2000).
27. Sherman, F., Fink, G. & Lawrence, C. *Methods in Yeast Genetics* (Cold Spring Harbor Laboratory Press, Cold Spring Harbor, 1974).
28. Sikorski, R. S. & Hieter, P. A system of shuttle vectors and yeast host strains designed for efficient manipulation of DNA in *Saccharomyces cerevisiae*. *Genetics* **122,** 19–27 (1989).
29. Schindler, T. *et al.* Crystal structure of Hck in complex with a Src family-selective tyrosine kinase inhibitor. *Mol. Cell* **3,** 639–648 (1999).
30. Biggins, S. *et al.* The conserved protein kinase Ipl1 regulates microtubule binding to kinetochores in budding yeast. *Genes Dev.* **13,** 532–544 (1999).

Supplementary information is available on *Nature*'s World-Wide Web site (http://www.nature.com) or as paper copy from the London editorial office of *Nature*.

Acknowledgements

We thank B. Schulman and E. Harlow for early characterization of mutant cyclin-dependent kinases; C. Co, V. Nguyen and J. Li for help with flow cytometry; D. Toczyski for help with the Coulter counter; A. Su for help with transcript array analysis; S. Jaspersen, C. Carroll, C. Takizawa, E. Weiss, S. Biggins, A. Szidon, A. Rudner, D. Kahne and A. Murray for helpful advice and reagents; E. O'Shea and R. Deshaies for strains and reagents. This work was supported by funding from the National Institute of Allergy and Immunology (K.M.S.), GlaxoWellcome (K.M.S. and J.L.W.), National Institute of General Medical Sciences (D.O.M.), National Institutes of Health (J.L.W.), Bristol-Myers Squibb (J.L.W.), Yamanouchi (J.L.W.) and a predoctoral fellowship from the National Science Foundation (J.A.U.). K.M.S. is a Pew, Searle, and a Sloan Foundation Scholar.

Correspondence and requests for material should be addressed to K.M.S. (e-mail: shokat@cmp.ucsf.edu).

The protein Aly links pre-messenger-RNA splicing to nuclear export in metazoans

Zhaolan Zhou*†, Ming-juan Luo*†, Katja Straesser‡, Jun Katahira‡, Ed Hurt‡ & Robin Reed*

** Department of Cell Biology, Harvard Medical School, Boston, Massachusetts 02115, USA*
‡ University of Heidelberg, Biochemie-Zentrum Heidelberg (BZH), Im Neuenheimer Feld 328, D-69120 Heidelberg, Germany

In metazoans, most pre-messenger RNAs contain introns that are removed by splicing. The spliced mRNAs are then exported to the cytoplasm. Recent studies showed that splicing promotes efficient mRNA export[1], but the mechanism for coupling these two processes is not known. Here we show that Aly, the metazoan homologue of the yeast mRNA export factor Yra1p (ref. 2), is recruited to messenger ribonucleoprotein (mRNP) complexes generated by splicing. In contrast, Aly does not associate with mRNPs assembled on identical mRNAs that already have no introns or with heterogenous nuclear RNP (hnRNP) complexes. Aly is recruited during spliceosome assembly, and then becomes tightly associated with the spliced mRNP. Aly shuttles between the nucleus and cytoplasm, and excess recombinant Aly increases both the rate and efficiency of mRNA export *in vivo*. Consistent with its splicing-dependent recruitment, Aly co-localizes with splicing factors in the nucleus. We conclude that splicing is required for efficient mRNA export as a result of coupling between the splicing and the mRNA export machineries.

Pre-mRNA splicing generates an mRNP complex distinct from that assembled on the identical mRNA lacking introns (Δi-mRNA)[1,3]. When these two types of complexes are injected into *Xenopus* oocyte nuclei, the mRNA in the spliced mRNP is exported to the cytoplasm more efficiently than that in the Δi-mRNP[1]. This

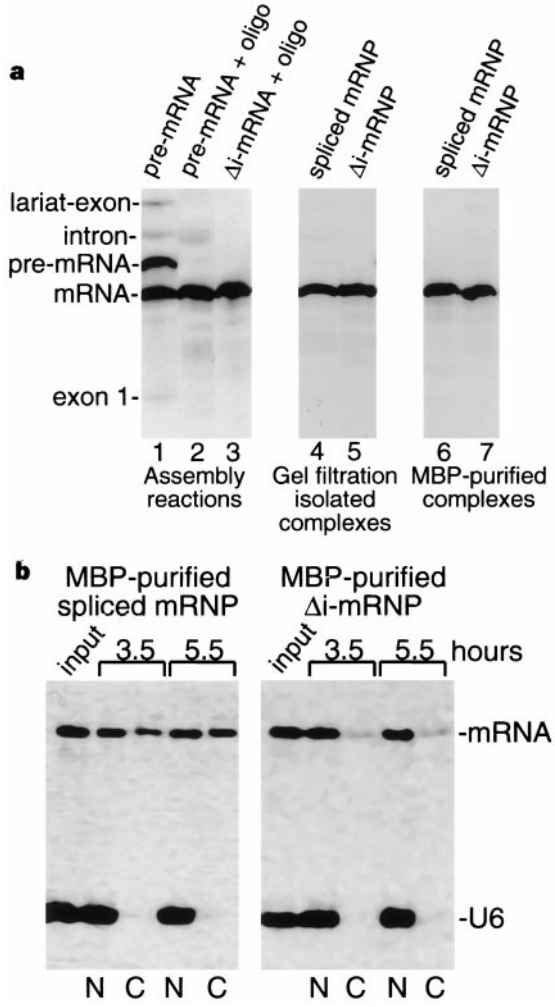

Figure 1 Purification of spliced messenger ribonucleoprotein (mRNP) that is functional in messenger RNA export. **a**, Maltose-binding protein (MBP)-affinity purification of spliced mRNP or Δi-mRNP. AdML pre-mRNA was incubated in nuclear extracts under splicing conditions for 60 minutes (lane 1). AdML pre-mRNA or Δi-mRNA was incubated under splicing conditions for 60 minutes, followed by addition, to both reactions, of a 12-mer oligonucleotide (5′-CTGCCTTTAGTG-3′) complementary to intron sequences immediately downstream from the 5′ splice site (lanes 2 and 3). Incubation was continued for 30 minutes, resulting in RNase H digestion of the pre-mRNA, intron lariat (a branched intermediate structure in the intron), and lariat-intermediate (compare lanes 1 and 2). There was no effect on the Δi-mRNA (lane 3). The complexes shown in lanes 2 and 3 were then isolated by gel filtration on Sephacryl S-500 (ref. 30). Total RNA isolated from the pooled fractions containing the mRNPs is shown in lanes 4 and 5. Gel filtration-isolated mRNPs were further purified by MBP-affinity chromatography. The total RNA in the elutions is shown in lanes 6 and 7. In negative control purification, no RNA or protein was detected in the elution, indicating the high specificity of the MBP-affinity purification strategy (data not shown). **b**, Export assays of the MBP-affinity-purified mRNPs. The spliced mRNP or Δi-mRNP (purified as in **a**) was mixed with U6 snRNA and injected into *Xenopus* oocyte nuclei. Oocytes were incubated at 18 °C for 0 (input), 3.5 or 5.5 hours, and the total RNA from the nucleus (N) or cytoplasm (C) was analysed.

† These authors contributed equally to this work.